Population transfer via stimulated Raman adiabatic passage in a solid

Hayato Goto and Kouichi Ichimura
Frontier Research Laboratory, Corporate Research and Development Center, Toshiba Corporation, 1, Komukai Toshiba-cho, Saiwai-ku, Kawasaki—shi, 212-8582, Japan

(Received 25 August 2006; published 13 November 2006)

We report experimental demonstration of population transfer via stimulated Raman adiabatic passage with a rare-earth-ion-doped crystal ($Pr^{3+}:Y_2SiO_5$). About 90% of population of a ground level is transferred to another ground level with two pulses whose width is shorter than the lifetime of the excited state. The dependence of transferred population on the delay time of the pulse sequence is also experimentally investigated. The delay-time dependence observed in our experiment is similar to that obtained by numerical simulation.

DOI: 10.1103/PhysRevA.74.053410 PACS number(s): 32.80.Qk, 03.67.Lx

I. INTRODUCTION

Adiabatic passage [1] is a good technique to manipulate quantum states. A number of implementations of quantum computation based on adiabatic passage have been proposed [2–8]. A typical example of adiabatic passage is laser-induced adiabatic passage via so-called dark (or trapped) states [9]. This is called stimulated Raman adiabatic passage (STIRAP) [10]. The STIRAP technique is a powerful tool for coherent and complete population transfer between two quantum states. Since the theoretical proposal [11], extensive theoretical investigations [12–17] and experimental demonstrations [18–23] of the population transfer via STIRAP have been reported. The STIRAP technique has also been applied to atom optics [24,25], state manipulation of laser-cooled atoms [26,27], and creation of superposition states [28–30]. The STIRAP process is closely related to electromagnetically induced transparency (EIT) [31,32] because both of them are based on the dark state or coherent population trapping (CPT) [9]. Light storage and quantum memory based on EIT and adiabatic passage [33–38] are also closely related to STIRAP.

In this paper, we report experimental demonstration of population transfer via STIRAP with a rare-earth-ion-doped crystal. The rare-earth-ion-doped crystals, such as $Pr^{3+}:Y_2SiO_5$ (hereafter Pr: YSO) used here, have the following good characteristics: sharp spectral structure unlike other solid materials [39], long coherence times of optical transitions (up to 6.4 ms) [40–43], and extremely long coherence times of hyperfine transitions (up to 33 s) [44–46]. Because of them, many implementations of quantum computation with rare-earth-ion-doped crystals have been proposed [47–53]. So far, EIT [44,54–56], light storage [57,58], and coherent state manipulation including quantum gate operations [59–62] have been realized with these crystals. To our knowledge, however, population transfer via STIRAP has not been experimentally investigated with these crystals. Moreover, experimental study of population transfer via STIRAP in solids has not been reported, while the realizations of EIT or, equivalently, CPT in solids have been reported [44,54–56,63–67] and techniques for population transfer via STIRAP in semiconductors have been theoretically proposed [68–70]. We experimentally investigate a three-level system in a Λ-type configuration, which is the typical system used for STIRAP [10], interacting with two laser pulses using Pr:YSO. The dependence of transferred population on the delay time of the pulse sequence is obtained experimentally and compared with numerical simulation.

This paper is organized as follows. In Sec. II, we briefly explain a simple theoretical model for STIRAP. In Sec. III, the experimental setup of our experiment is illustrated. In Sec. IV, experimental methods are presented. In Sec. V, experimental results are presented. In Sec. VI, we discuss experimental results comparing numerical simulation results. The conclusion is presented in Sec. VII.

II. BASIC THEORY FOR STIRAP

A three-level system in a Λ-type configuration interacting with two laser fields is depicted in Fig. 1. This is the typical system for STIRAP [10] and EIT [31].

The Hamiltonian in the rotating-wave approximation is given by [10]

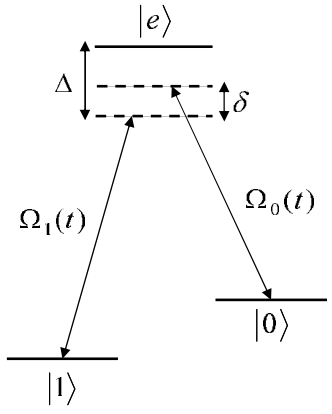

FIG. 1. Three-level system in a Λ configuration. Δ is the one-photon detuning from the $|1\rangle$-$|e\rangle$ transition. δ is the two-photon detuning from the $|0\rangle$-$|1\rangle$ transition. $\Omega_0(t)$ and $\Omega_1(t)$ are the Rabi frequencies corresponding to the $|0\rangle$-$|e\rangle$ and $|1\rangle$-$|e\rangle$ transitions, respectively.

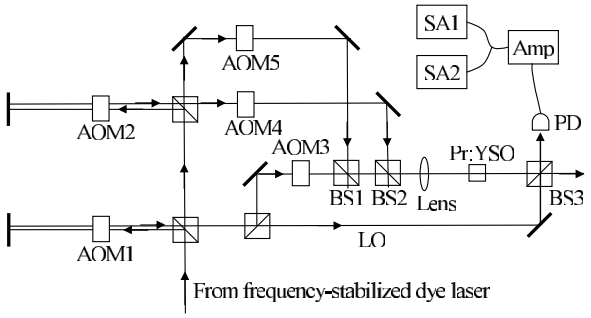

FIG. 2. Schematic of the experimental setup. AOM: acousto-optic modulator. BS: beam splitter. PD: photodiode. Amp: amplifier. SA: spectrum analyzer. LO: local oscillator.

$$H(t) = \hbar\delta|0\rangle\langle 0| + \hbar\Delta|e\rangle\langle e| + i\frac{\hbar}{2}\Omega_0(t)(|e\rangle\langle 0| - |0\rangle\langle e|)$$

$$+ i\frac{\hbar}{2}\Omega_1(t)(|e\rangle\langle 1| - |1\rangle\langle e|), \quad (1)$$

where Δ is the one-photon detuning from the $|1\rangle$-$|e\rangle$ transition, δ is the two-photon detuning from the $|0\rangle$-$|1\rangle$ transition, and $\Omega_0(t)$ and $\Omega_1(t)$ are the Rabi frequencies corresponding to the $|0\rangle$-$|e\rangle$ and $|1\rangle$-$|e\rangle$ transitions, respectively (we have assumed they are real). In this section, we consider the case of two-photon resonance, that is, $\delta=0$. Since the STIRAP process is sensitive to the two-photon detuning [16,17], we take the two-photon detuning into account in Sec. VI. There is a dark state [9], which is the zero-eigenvalue eigenstate of the Hamiltonian, expressed as

$$|D(t)\rangle = \frac{\Omega_1(t)|0\rangle - \Omega_0(t)|1\rangle}{\sqrt{\Omega_0(t)^2 + \Omega_1(t)^2}}. \quad (2)$$

If the system is initially in the dark state and the variation of the Hamiltonian is sufficiently slow, the system adiabatically follows the dark state. This is the STIRAP process. By using the STIRAP technique, we can achieve efficient population transfer from $|0\rangle$ to $|1\rangle$ as explained below. To achieve this population transfer, we use partially overlapped laser pulses in the *counterintuitive* order in which a pulse initially couples the two empty states, $|1\rangle$ and $|e\rangle$, and next another pulse couples $|0\rangle$ and $|e\rangle$. Then, the dark state varies from $|0\rangle$ to $|1\rangle$. Therefore if the system is initially in $|0\rangle$, the population is transferred from $|0\rangle$ to $|1\rangle$ by the STIRAP process. The adiabatic condition is that the Rabi frequencies are sufficiently larger than the inverse of the pulse width [10].

III. EXPERIMENTAL SETUP

The experimental setup is shown in Fig. 2.

The light source is a ring dye (Rhodamine 6G) laser (Coherent 699-29) pumped by an argon ion laser (Coherent INNOVA400). The frequency jitter is reduced to several kHz over 15 ms by locking to the resonance frequency of an external stable cavity using the Pound-Drever-Hall method [71]. The frequency-stabilized laser is split into three beams. As explained in the next section, the laser fields of three frequencies are required to prepare the ionic state appropriately. The frequencies of the three fields are set to ν_0, $\nu_1 = \nu_0 + 10.2$ MHz, and $\nu_2 = \nu_0 + 36.9$ MHz ($\nu_0 \sim 494.72$ THz; see Fig. 4) by two acousto-optic modulators (AOM1 and AOM2 in Fig. 2). The waveforms of the three beams are controlled with the other three AOMs. The three beams are combined with two beam splitters (BS1 and BS2 in Fig. 2). The combined beam is tightly focused on the sample in a cryostat with a 100-mm-focal-length lens. The beam radius (e^{-2} in intensity) on the sample is about 16 μm. The sample is a 3-mm-thick Pr:YSO crystal whose Pr^{3+} concentration is about 0.05 at. %. The b axis is parallel to the direction of the beam. The polarization of the field is adjusted to obtain maximum absorption. The sample is kept at 4 K. The transmitted light interferes with a local oscillator and the transmission intensity is measured by heterodyne detection. The output of the photodiode is amplified by a wide band amplifier and input to two spectrum analyzers (SAs). The resolution and video bandwidths of the SAs are set to 1 MHz. The outputs of the SAs are input to a digital oscilloscope. All the data are accumulated over 64 cycles by the oscilloscope. The duration of one cycle is 24 ms (see the next section).

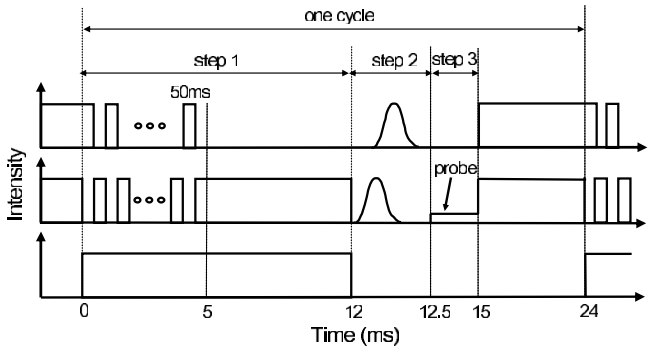

FIG. 3. waveforms of the three fields used in the experiment. The top, middle, and bottom diagrams correspond to the fields of frequencies ν_0, ν_1, and ν_2, respectively. This figure shows the case where the order of the pulse sequence is counterintuitive and where the population of $|1\rangle$ is measured by measuring the transmittance of the probe of ν_1.

IV. EXPERIMENTAL METHODS

A. waveforms of the three laser fields

In the present experiment, we use three laser fields of frequencies ν_0, ν_1, and ν_2. (As mentioned in Sec. III, $\nu_0 \sim 494.72$ THz, $\nu_1 = \nu_0 + 10.2$ MHz, and $\nu_2 = \nu_0 + 36.9$ MHz.) The waveforms of the fields are shown in Fig. 3. The maximal intensities of the fields are set to about 10 μW. The process of the experiment consists of the following three steps: step 1 is preparation of the ionic state, including initialization of the ionic state to $|0\rangle$, by optical pumping with the above three fields; step 2 is population transfer from $|0\rangle$ to $|1\rangle$ with two Gaussian pulses of frequencies ν_0 and ν_1; and step 3 is measurement of the population with a weak probe field of ν_0 or ν_1. The details of the steps are described in the following.

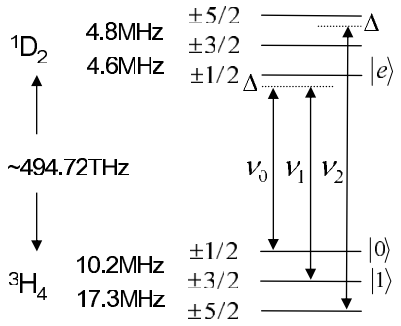

FIG. 4. Energy-level diagram of Pr^{3+} ions doped in a YSO crystal. Δ denotes one-photon detunings. Two-photon detunings are ignored (not shown).

B. Step 1: Initialization of ionic state

The energy-level diagram of Pr^{3+} ions doped in a YSO crystal is shown in Fig. 4 [72]. We use the $^3H_4$-$^1D_2$ transition of site-I Pr^{3+} ions in YSO. As shown in Fig. 4, $|^3H_4, \pm 1/2\rangle$, $|^3H_4, \pm 3/2\rangle$, and $|^1D_2, \pm 1/2\rangle$ are regarded as $|0\rangle$, $|1\rangle$, and $|e\rangle$, respectively, in Fig. 1. The ions used for the demonstration of population transfer via STIRAP are only those whose $|^3H_4, \pm 1/2\rangle$-$|^1D_2, \pm 1/2\rangle$, $|^3H_4, \pm 3/2\rangle$-$|^1D_2, \pm 1/2\rangle$, and $|^3H_4, \pm 5/2\rangle$-$|^1D_2, \pm 5/2\rangle$ transitions are nearly resonant with the fields of ν_0, ν_1, and ν_2, respectively, as shown in Fig. 4. This choice of the levels is suitable for the following reasons.

(1) The inhomogeneous linewidth of the $|^3H_4, \pm 1/2\rangle$-$|^3H_4, \pm 3/2\rangle$ transition is relatively narrow (~30 kHz) [73].

(2) The transition dipole moments of the $|^3H_4, \pm 1/2\rangle$-$|^1D_2, \pm 1/2\rangle$, $|^3H_4, \pm 3/2\rangle$-$|^1D_2, \pm 1/2\rangle$, and $|^3H_4, \pm 5/2\rangle$-$|^1D_2, \pm 5/2\rangle$ transitions are relatively large [72].

(3) The appropriate preparation of the ionic state can be achieved by optical pumping as explained below.

Because of the inhomogeneous broadening of the optical transitions (~10 GHz [73,74]), there are many unnecessary ions whose $|^3H_4, \pm 1/2\rangle$-$|^1D_2, \pm 1/2\rangle$, $|^3H_4, \pm 3/2\rangle$-$|^1D_2, \pm 1/2\rangle$, and $|^3H_4, \pm 5/2\rangle$-$|^1D_2, \pm 1/2\rangle$ transitions are far off-resonant with the fields of ν_0, ν_1, and ν_2, respectively, but which have at least a transition interacting with a field. These unnecessary ions can be removed by optical pumping with the three fields. The role of the part from $t=0$ to 5 ms in step 1 in Fig. 3 is this pumping. After the pumping, the population of the unnecessary ions is concentrated on the ground states decoupled from any excited states. In this interval, the fields of ν_0 and ν_1 are applied as square pulse sequences so that CPT does not prevent the pumping. The other part of step 1 concentrates the population of the ions used for the demonstration on $|0\rangle$ by optical pumping.

C. Step 2: Population transfer with two pulses

A two-pulse sequence for population transfer comes just after the preparation and initialization of the ionic state, as shown in Fig. 3. The pulse shape is set as $\Omega_j(t) \propto \exp[-(t-t_j)^2/T^2]$ $(j=0,1)$, where $\Omega_j(t)$ denotes the Rabi frequency corresponding to the $|j\rangle$-$|e\rangle$ transition, t_j is the time at which the peak of $\Omega_j(t)$ comes, and T is the pulse width. T is set to 30 μs in the present experiment.

D. Step 3: Measurement of population

In step 3 (see Fig. 3), a weak probe field of frequency ν_0 (ν_1) is injected to estimate the population of $|0\rangle$ ($|1\rangle$). The intensities of the probes are about 0.1 μW (about 1/100 of the maximal intensities of the fields). The transmission intensities are measured by heterodyne detection (see Sec. III). Here, we describe in detail how the population is estimated from the measured transmittance. We first explain the estimation of the population of $|1\rangle$. The transmittance is obtained from the comparison of the measured transmission intensity with that in the case of no absorption. The transmission intensity in the case of no absorption can be measured by injecting only the field of frequency ν_1, since the crystal transmits the incident light without absorption owing to hole burning. A single optical transition (from $|1\rangle$ to $|e\rangle$) is excited by the probe of ν_1. The transmittance, $T_p(t)$, of the probe can be calculated by solving a master equation and Maxwell equations for an inhomogeneously broadened two-level medium [75]:

$$\frac{\partial}{\partial t}\rho(t,z,\Delta) = -\frac{i}{\hbar}[H(t,z,\Delta),\rho(t,z,\Delta)] + L[\rho(t,z,\Delta)], \quad (3)$$

$$\frac{\partial}{\partial z}\Omega_p(t,z) = i\mu^2 NC \int \rho_{e,1}(t,z,\Delta)P(\Delta)d\Delta, \quad (4)$$

with

$$\rho(t,z,\Delta) = \sum_{k,l=1,e} \rho_{k,l}(t,z,\Delta)|k\rangle\langle l| = \begin{pmatrix} \rho_{1,1}(t,z,\Delta) & \rho_{1,e}(t,z,\Delta) \\ \rho_{e,1}(t,z,\Delta) & \rho_{e,e}(t,z,\Delta) \end{pmatrix}, \quad (5)$$

$$H(t,z,\Delta) = \hbar\Delta|e\rangle\langle e| + i\frac{\hbar}{2}[\Omega_p(t,z)|e\rangle\langle 1| - \Omega_p^*(t,z)|1\rangle\langle e|], \quad (6)$$

$$L[\rho(t,z,\Delta)] = \begin{pmatrix} p\gamma\rho_{e,e}(t,z,\Delta) & -\gamma_p\rho_{1,e}(t,z,\Delta) \\ -\gamma_p\rho_{e,1}(t,z,\Delta) & -\gamma\rho_{e,e}(t,z,\Delta) \end{pmatrix}, \quad (7)$$

$$C = \frac{2\pi}{\hbar\epsilon_0 n\lambda}, \quad (8)$$

$$\rho(0,z,\Delta) = \begin{pmatrix} 1 & 0 \\ 0 & 0 \end{pmatrix}, \quad (9)$$

$$\Omega_p(t,0) = \Omega_p^{(0)}. \quad (10)$$

Here, the z axis is set along the direction of the light beam; $\rho(t,z,\Delta)$ is the density matrix describing the states of the two-level systems with detuning Δ and at position z; $\Omega_p(t,z)$ is the Rabi frequency of the $|1\rangle$-$|e\rangle$ transition of the ions at z; μ is the transition dipole moment of the $|1\rangle$-$|e\rangle$ transition; N is the ionic density per unit volume per unit detuning frequency; $P(\Delta)$ is the population distribution of $|1\rangle$ with respect to Δ just before the probe is injected; γ and γ_p are the population dumping rate and the dephasing rate, respectively, for optical transitions; p is the probability that the ions decay

from $|e\rangle$ to $|1\rangle$; ϵ_0 is the permittivity of vacuum; n is the refractive index of the YSO crystal; λ is the laser wavelength; and $\Omega_p^{(0)}$ is the Rabi frequency corresponding to the constant incident intensity of the probe. What is to be estimated is the population distribution $P(\Delta)$. It should be noted that the transmittance of the probe depends only on the population of $|1\rangle$, neither on the population of the other ground states nor the coherence between the ground states, if the excited state is unpopulated. In the present experiment, $\lambda=606$ nm and $n=1.8$ [76]. The transmittance, $T_p(t)$, of the probe is given by $|\Omega_p(t,l)|^2/|\Omega_p^{(0)}|^2$, where l is the crystal length (3 mm). In our calculation, γ and γ_p are set to 6 and 9 kHz, respectively [74]. p is set to 0.40 by assuming that the probability is proportional to the oscillator strength as pointed out in Ref. [72]. The uncertainties with respect to the decay are unimportant since the data in short time (20 μs) are used for the estimation. μ is set to 1.7×10^{-32} Cm [72]. Thus if N and $\Omega_p^{(0)}$ are known, $P(\Delta)$ can be estimated by fitting the calculated $T_p(t)$ to the measured $T_p(t)$.

In the case of the estimation of the population of $|0\rangle$ with the probe of frequency ν_0, μ and p are reset as follows: $\mu=2.0\times10^{-32}$ Cm [72] and $p=0.55$.

N and $\Omega_p^{(0)}$ are determined from $T_p(t)$ measured in a supplementary experiment in which the ionic state is initialized to $|0\rangle$ or $|1\rangle$ and the probe is injected 100 μs after the initialization without step 2 (without the two-pulse sequence), where $P(\Delta)=1$ is assumed. The initialization to $|1\rangle$ is performed by exchanging the waveforms of the fields of frequencies ν_0 and ν_1.

V. RESULTS

A. Initialization

To determine N and $\Omega_p^{(0)}$, we first perform the experiment in which the ionic state is initialized to $|0\rangle$ or $|1\rangle$ and the probe is injected 100 μs after the initialization without step 2 (without the two-pulse sequence).

The experimental results are shown in Fig. 5. Figures 5(a) and 5(b) correspond to the cases where the ionic state is initialized to $|0\rangle$ and $|1\rangle$, respectively. The circles and the triangles show the measured $T_p(t)$ for the probes of frequencies ν_0 and ν_1, respectively. The origin of time is roughly set so that the intensities of the probes reach the plateau at $t=0$. The data are accumulated over 64 cycles as mentioned in Sec. III. The curves are the theoretical fits using the least-squares method, where the curves are numerically calculated with Eqs. (3)–(10) assuming $P(\Delta)=1$. To take the bandwidth of the SAs into account, the calculated curves are averaged at each time over 1.6 and 1.2 μs on a linear scale for SA1 and SA2, respectively, where SA1 and SA2 are used for the probes of ν_0 and ν_1, respectively. In addition, to take into account the jitter of the time at which the probe rises, the calculated curves are averaged at each time over 1.2 μs on a log scale. The fitting parameters in the case of Fig. 5(a) are N and $\Omega_p^{(0)}$. The result of the fitting is as follows: $N=0.074$ μm^{-3} kHz^{-1}; $\Omega_p^{(0)}/2\pi=11$ kHz. On the other hand, the fitting parameter in the case of Fig. 5(b) is only $\Omega_p^{(0)}$, and

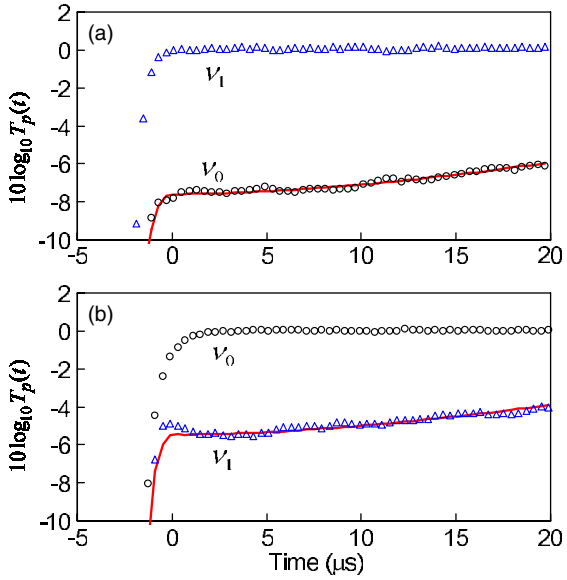

FIG. 5. (Color online) The measured transmittance, $T_p(t)$, of the probe for estimation of N and $\Omega_p^{(0)}$. (a) and (b) show the results in the cases where the ionic state is initialized to $|0\rangle$ and $|1\rangle$, respectively. The circles and the triangles show the measured $T_p(t)$ for the probes of frequencies ν_0 and ν_1, respectively. The curves are the theoretical fits.

N is set to 0.074 μm^{-3} kHz^{-1}. The result of the fitting in this case is $\Omega_p^{(0)}/2\pi=11$ kHz.

B. Population transfer

Next, we report the experimental results of the case where the two-pulse sequence is applied. The delay time, $T_d\equiv t_0-t_1$, of the pulse sequence is set to $T_d=-T$, $-0.5T,\ldots,2.5T$. Here, as mentioned in Sec. IV, the Rabi frequency corresponding to the $|j\rangle$-$|e\rangle$ transition is set as $\Omega_j(t)\propto\exp[-(t-t_j)^2/T^2]$ $(j=0,1)$ and T is set to 30 μs.

The measured transmittances, $T_p(t)$, of the probes are shown in Fig. 6. The circles and the triangles show the measured $T_p(t)$ for the probes of frequencies ν_0 and ν_1, respectively. The curves are the theoretical fits, where the curves are numerically calculated with Eqs. (3)–(10). In these calculations, N and $\Omega_p^{(0)}$ are set to the values obtained above: $N=0.074$ μm^{-3} kHz^{-1} and $\Omega_p^{(0)}/2\pi=11$ kHz. The function forms of the population distribution, $P(\Delta)$, are assumed as shown in Table I. The fitting parameters for the above fitting are the parameters, a_1, a_2, a_3, and a_4, determining $P(\Delta)$. The population distributions obtained by the fitting are shown in Fig. 7. We assume a complicated function form only for the population of $|1\rangle$ in the case where $T_d=-T$, to obtain the good fit. The reason why $P(\Delta)$ in this case has a dip is discussed in the next section.

The delay-time dependence of the population of the ions with zero detuning ($\Delta=0$) is shown in Fig. 8(a). This is the main result of the present work.

VI. DISCUSSION

We first discuss the results shown in Fig. 5. The transmittance of the probe of frequency ν_1 (ν_0) in the case of the

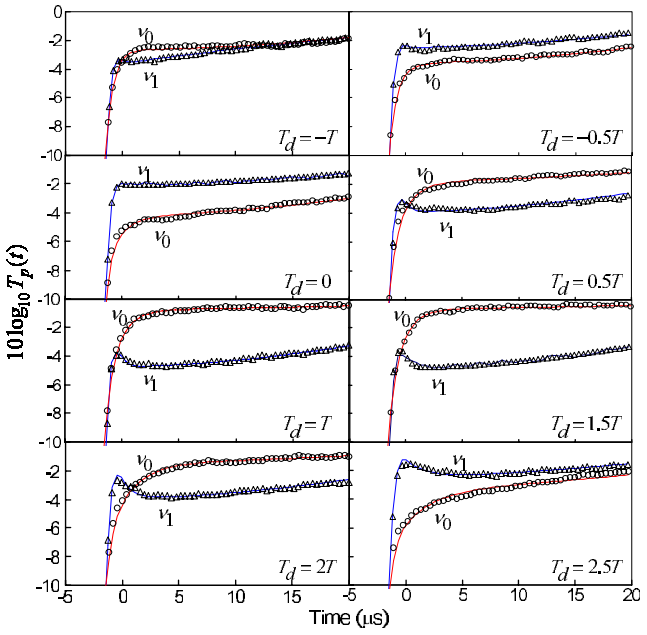

FIG. 6. (Color online) The measured transmittance, $T_p(t)$, of the probe in the experiment of population transfer by the two-pulse sequence. T_d and T denote the delay time of the pulse sequence and the pulse width, respectively (see the text for these definitions). The circles and the triangles show the measured $T_p(t)$ for the probes of frequencies ν_0 and ν_1, respectively. The curves are the theoretical fits.

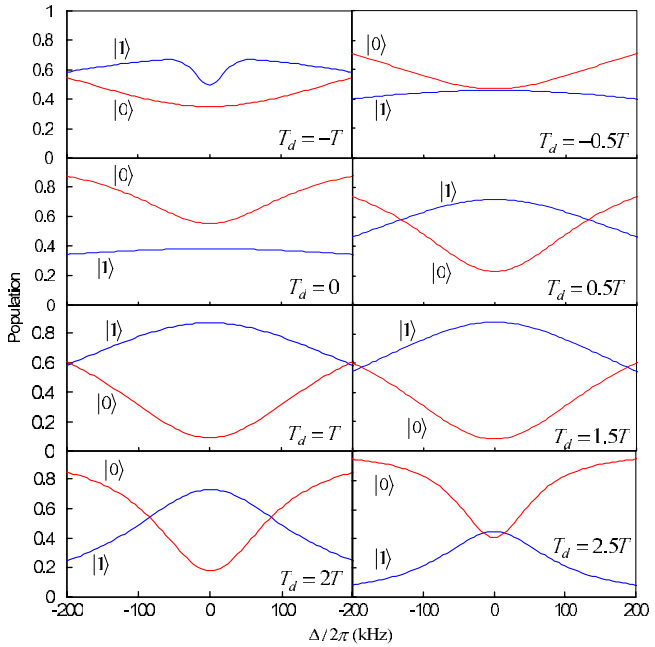

FIG. 7. (Color online) The population distributions, $P(\Delta)$, in the experiment of population transfer by the two-pulse sequence. These are obtained by the fitting shown in Fig. 6. T_d and T denote the delay time of the pulse sequence and the pulse width, respectively (see the text for these definitions).

initialization to $|0\rangle$ ($|1\rangle$) is nearly equal to unity as expected. In addition to this, the fact that the experimental result in the case of the initialization to $|1\rangle$ is well fitted to a theoretical curve with N determined by the result in the case of the initialization to $|0\rangle$ indicates that the initialization processes were successfully performed.

Second, we estimate the peak Rabi frequencies, $\Omega_0^{(0)}$ and $\Omega_1^{(0)}$, for the pulses of frequencies ν_0 and ν_1, from the fitting results of $\Omega_p^{(0)}$. From the transmission intensities in the case of no absorption (measured by injecting only one field as explained in Sec. IV), the maximal intensities of the fields of frequencies ν_0 and ν_1 are about 100 times and 140 times larger than the intensities of the probes of ν_0 and ν_1, respectively. Therefore the estimated values of $\Omega_0^{(0)}/2\pi$ and $\Omega_1^{(0)}/2\pi$ are 110 and 130 kHz, respectively. Since both $\Omega_0^{(0)}$ and $\Omega_1^{(0)}$ are much larger than $T^{-1} \simeq 30$ kHz, the adiabatic condition is satisfied.

Next, we discuss the results shown in Fig. 8. First of all, it should be noted that the delay-time dependence of

TABLE I. The function forms of the population distribution, $P(\Delta)$, for the fitting shown in Fig. 6. a_1, a_2, a_3 and a_4 are the fitting parameters. The population distributions obtained by the fitting are shown in Fig. 7.

	$P(\Delta)$
$\|0\rangle$	$1-a_1[a_2^2/(\Delta^2+a_2^2)]$
$\|1\rangle$ $(T_d \neq -T)$	$a_1[a_2^2/(\Delta^2+a_2^2)]$
$\|1\rangle$ $(T_d=-T)$	$a_1[a_2^2/(\Delta^2+a_2^2)]-a_3 e^{-\Delta^2/a_4^2}$

population transfer shown in Fig. 8(a) is a characteristic signature of the STIRAP process [10]. Figure 8(a) shows that about 90% of the population was transferred from $|0\rangle$ to $|1\rangle$ when $T_d=T$ and $T_d=1.5T$ (the case of the counterintuitive order). The fact that large population was transferred with the pulses shorter than the lifetime (164 μs [74]) of the excited state indicates that this population transfer was due to

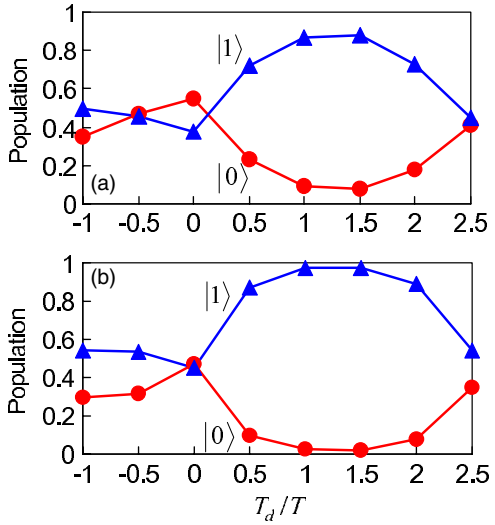

FIG. 8. (Color online) The delay-time dependence of the population of the ions with zero detuning ($\Delta=0$). The circles and the triangles correspond to $|0\rangle$ and $|1\rangle$, respectively. (a) The experimental result. The population was estimated by the fitting shown in Figs. 6 and 7. (b) The simulation result. The population was calculated by a model explained in Sec. VI.

STIRAP, not optical pumping. Figure 8(a) also shows the insensitivity of STIRAP to the delay time, which is a merit of STIRAP. We compare the experimental results with numerical simulation. The simulation result is shown in Fig. 8(b). The model for the simulation is as follows. We solve numerically the following master equation:

$$\frac{d}{dt}\rho(t,\delta) = -\frac{i}{\hbar}[H(t),\rho(t,\delta)] + L[\rho(t,\delta)], \tag{11}$$

where $H(t)$ is the Hamiltonian given by Eq. (1) with $\Delta=0$ and

$$\rho(t,\delta) = \sum_{k,l=0,1,e} \rho_{k,l}(t,\delta)|k\rangle\langle l| = \begin{pmatrix} \rho_{0,0}(t,\delta) & \rho_{0,1}(t,\delta) & \rho_{0,e}(t,\delta) \\ \rho_{1,0}(t,\delta) & \rho_{1,1}(t,\delta) & \rho_{1,e}(t,\delta) \\ \rho_{e,0}(t,\delta) & \rho_{e,1}(t,\delta) & \rho_{e,e}(t,\delta) \end{pmatrix}, \tag{12}$$

$$L[\rho(t,\delta)] = \begin{pmatrix} p_0\gamma\rho_{e,e}(t,\delta) & -\gamma_p'\rho_{0,1}(t,\delta) & -\gamma_p\rho_{0,e}(t,\delta) \\ -\gamma_p'\rho_{1,0}(t,\delta) & p_1\gamma\rho_{e,e}(t,\delta) & -\gamma_p\rho_{1,e}(t,\delta) \\ -\gamma_p\rho_{e,0}(t,\delta) & -\gamma_p\rho_{e,1}(t,\delta) & -\gamma\rho_{e,e}(t,\delta) \end{pmatrix}, \tag{13}$$

$$\rho(0,\delta) = \begin{pmatrix} 1 & 0 & 0 \\ 0 & 0 & 0 \\ 0 & 0 & 0 \end{pmatrix}. \tag{14}$$

Here, δ is the two-photon detuning from the $|0\rangle$-$|1\rangle$ transition, γ is the population dumping rate, γ_p and γ_p' are the dephasing rates for optical and hyperfine transitions, respectively, and p_j $(j=0,1)$ is the probability that the ions decay from $|e\rangle$ to $|j\rangle$. These parameters are set as follows: $\gamma=6$ kHz; $\gamma_p=9$ kHz; $\gamma_p'=2$ kHz; $p_0=0.55$; and $p_1=0.40$ [44,72,74]. The Rabi frequencies are set as $\Omega_j(t)=\Omega_j^{(0)}\exp[-(t-t_j)^2/T^2]$ $(j=0,1)$, where $T=30$ μs, $t_1=4T$, $t_0=t_1+T_d$ $(T_d=-T,-0.5T,\ldots,2.5T)$, $\Omega_0^{(0)}/2\pi=110$ kHz, and $\Omega_1^{(0)}/2\pi=130$ kHz. The calculation is performed from $t=0$ to $t_f=500$ μs. The calculation result shown in Fig. 8(b) is obtained by averaging $\rho_{0,0}(t_f,\delta)$ and $\rho_{1,1}(t_f,\delta)$ with respect to δ. The two-photon-detuning distribution, $W(\delta)$, of the ions, which is due to the inhomogeneous broadening of the $|0\rangle$-$|1\rangle$ transition, is assumed as follows [73]:

$$W(\delta) = \begin{cases} 1 & \cdots \quad |\delta|/2\pi \leqslant 15 \text{ kHz}, \\ 0 & \cdots \quad \text{otherwise}. \end{cases} \tag{15}$$

The delay-time dependence of the population obtained by the simulation is similar to that by the experiment. The calculated population of $|1\rangle$ ($|0\rangle$) is a little larger (smaller) than the experimental one. This discrepancy may be due to the neglect of the laser beam profile [77]. Since each beam has a Gaussian profile, which has been neglected so far for simplicity, the Rabi frequencies depend on the position of the ions. Therefore the present experimental results show the average with respect to the position-dependent Rabi frequencies. As a result, the efficiency of the population transfer estimated from the experimental results becomes lower than that from the simulation because the efficiency for the ions far from the axis of the beams is lower than that for the ions near the axis.

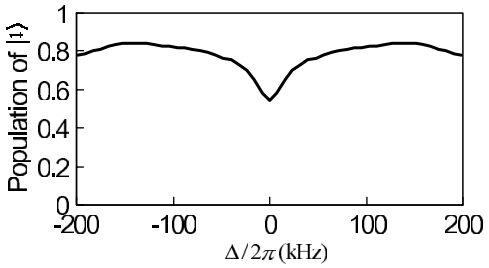

FIG. 9. The simulation result of the population distribution of $|1\rangle$ in the case where $T_d=-T$.

Finally, we discuss the reason why the population distribution of $|1\rangle$ in the case where $T_d=-T$ has a dip at $\Delta=0$. The population distribution in this case is calculated by the simulation used to obtain Fig. 8(b). The result is shown in Fig. 9. The calculated population distribution has also a dip at $\Delta=0$. The physical interpretation of the dip is probably as follows. In this case, where the order of the pulse sequence is "intuitive," the ions with small detuning are excited by the pulses to the excited state and the population transfer is due to optical pumping. Since the pulse resonating with the $|1\rangle$-$|e\rangle$ transtion, which reduces the population of $|1\rangle$ by optical pumping, comes after the pulse resonating with the $|0\rangle$-$|e\rangle$ transtion, which induces the population transfer from $|0\rangle$ to $|1\rangle$, the population transfer due to the optical pumping is not efficient. On the other hand, the ions with relatively large detuning are not excited very much and the population transfer is due to a coherent process such as off-resonant Raman transition. As a result, the transferred population for the ions with large detuning becomes larger than that for the ions with small detuning. This is probably the reason for the appearance of the dip.

VII. CONCLUSION

In summary, we have investigated the three-level system in a Λ-type configuration interacting with two laser pulses using a rare-earth-ion-doped crystal (Pr:YSO). The experimental demonstration of population transfer via STIRAP in a solid has been reported. It has been confirmed that about 90% of population was transferred from a ground state to another with shorter pulses than the lifetime of the excited state. Moreover, the delay-time dependence of the population obtained by the experiment shows a characteristic signature of the STIRAP process and is similar to that by numerical simulation.

This population transfer via STIRAP is the simplest quantum-state manipulation by the STIRAP technique. The experiment presented here is the first step toward more complicated quantum-state manipulations of rare-earth ions in a crystal by the STIRAP technique.

[1] L. I. Schiff, *Quantum Mechanics* (McGraw-Hill, New York, 1955).
[2] T. Pellizzari, S. A. Gardiner, J. I. Cirac, and P. Zoller, Phys. Rev. Lett. **75**, 3788 (1995).
[3] L.-M. Duan, J. I. Cirac, and P. Zoller, Science **292**, 1695 (2001).
[4] M. S. Shahriar *et al.*, Opt. Commun. **195**, 411 (2001).
[5] Z. Kis and F. Renzoni, Phys. Rev. A **65**, 032318 (2002).
[6] J. Pachos and H. Walther, Phys. Rev. Lett. **89**, 187903 (2002).
[7] H. Goto and K. Ichimura, Phys. Rev. A **70**, 012305 (2004).
[8] N. Sangouard, X. Lacour, S. Guérin, and H. R. Jauslin, Phys. Rev. A **72**, 062309 (2005).
[9] E. Arimondo, *Progress in Optics*, edited by E. Wolf (Elsevier Science, Amsterdam, 1996), Vol. 35, p. 257.
[10] K. Bergmann, H. Theuer, and B. W. Shore, Rev. Mod. Phys. **70**, 1003 (1998).
[11] J. Oreg, F. T. Hioe, and J. H. Eberly, Phys. Rev. A **29**, 690 (1984).
[12] J. R. Kuklinski, U. Gaubatz, F. T. Hioe, and K. Bergmann, Phys. Rev. A **40**, 6741 (1989).
[13] B. W. Shore, J. Martin, M. P. Fewell, and K. Bergmann, Phys. Rev. A **52**, 566 (1995).
[14] J. Martin, B. W. Shore, and K. Bergmann, Phys. Rev. A **52**, 583 (1995).
[15] N. V. Vitanov and S. Stenholm, Opt. Commun. **135**, 394 (1997).
[16] V. I. Romanenko and L. P. Yatsenko, Opt. Commun. **140**, 231 (1997).
[17] G. G. Grigoryan and Y. T. Pashayan, Opt. Commun. **198**, 107 (2001).
[18] U. Gaubatz *et al.*, Chem. Phys. Lett. **149**, 463 (1988).
[19] U. Gaubatz, P. Rudechi, S. Schiemann, and K. Bergmann, J. Chem. Phys. **92**, 5363 (1990).
[20] P. Pillet, C. Valentin, R.-L. Yuan, and J. Yu, Phys. Rev. A **48**, 845 (1993).
[21] T. Halfmann and K. Bergmann, J. Chem. Phys. **104**, 7068 (1996).
[22] J. Martin, B. W. Shore, and K. Bergmann, Phys. Rev. A **54**, 1556 (1996).
[23] T. Peters, L. P. Yatsenko, and T. Halfmann, Phys. Rev. Lett. **95**, 103601 (2005).
[24] M. Weitz, B. C. Young, and S. Chu, Phys. Rev. Lett. **73**, 2563 (1994).
[25] H. Theuer, R. G. Unanyan, C. Habscheid, K. Klein, and K. Bergmann, Opt. Express **4**, 77 (1999).
[26] L. S. Goldner, C. Gerz, R. J. C. Spreeuw, S. L. Rolston, C. I. Westbrook, W. D. Phillips, P. Marte, and P. Zoller, Phys. Rev. Lett. **72**, 997 (1994).
[27] S. Kulin, B. Saubamea, E. Peik, J. Lawall, T. W. Hijmans, M. Leduc, and C. Cohen-Tannoudji, Phys. Rev. Lett. **78**, 4185 (1997).
[28] R. Unanyan, M. Fleischhauer, B. W. Shore, and K. Bergmann, Opt. Commun. **155**, 144 (1998).
[29] F. Vewinger, M. Heinz, R. GarciaFernandez, N. V. Vitanov, and K. Bergmann, Phys. Rev. Lett. **91**, 213001 (2003).
[30] V. A. Sautenkov, C. Y. Ye, Y. V. Rostovtsev, G. R. Welch, and M. O. Scully, Phys. Rev. A **70**, 033406 (2004).
[31] S. E. Harris, Phys. Today **50**, 36 (1997).
[32] M. Fleischhauer, A. Imamoglu, and J. P. Marangos, Rev. Mod. Phys. **77**, 633 (2005).
[33] M. Fleischhauer and M. D. Lukin, Phys. Rev. Lett. **84**, 5094 (2000).
[34] D. F. Phillips, A. Fleischhauer, A. Mair, R. L. Walsworth, and M. D. Lukin, Phys. Rev. Lett. **86**, 783 (2000).
[35] C. Liu, Z. Dutton, C. H. Behroozi, and L. V. Hau, Nature (London) **409**, 490 (2001).
[36] M. Fleischhauer and M. D. Lukin, Phys. Rev. A **65**, 022314 (2002).
[37] M. D. Lukin, Rev. Mod. Phys. **75**, 457 (2003).
[38] T. Chaneliere, Nature (London) **438**, 833 (2005).
[39] R. M. Macfarlane and R. M. Shelby, *Spectroscopy of Solids Containing Rare-Earth Ions*, edited by A. A. Kaplyanskii and R. M. Macfarlane (North-Holland, Amsterdam, 1987), Chap. 3.
[40] R. Yano, M. Mitsunaga, and N. Uesugi, Opt. Lett. **16**, 1884 (1991).
[41] R. W. Equall, Y. Sun, R. L. Cone, and R. M. Macfarlane, Phys. Rev. Lett. **72**, 2179 (1994).
[42] Y. Sun, C. W. Thiel, R. L. Cone, R. W. Equall, and R. L. Hutcheson, J. Lumin. **98**, 281 (2002).
[43] R. M. Macfarlane, J. Lumin. **100**, 1 (2002).
[44] B. S. Ham, M. S. Shahriar, M. K. Kim, and P. R. Hemmer, Opt. Lett. **22**, 1849 (1997).
[45] E. Fraval, M. J. Sellars, and J. J. Longdell, Phys. Rev. Lett. **92**, 077601 (2004).
[46] E. Fraval, M. J. Sellars, and J. J. Longdell, Phys. Rev. Lett. **95**, 030506 (2005).
[47] K. Ichimura, Opt. Commun. **196**, 119 (2001).
[48] M. S. Shahriar *et al.*, Opt. Commun. **195**, 411 (2001).
[49] N. Ohlsson, R. K. Mohan, and S. Kröll, Opt. Commun. **201**, 71 (2002).
[50] J. Wesenberg and K. Mølmer, Phys. Rev. A **68**, 012320 (2003).
[51] I. Roos and K. Mølmer, Phys. Rev. A **69**, 022321 (2004).
[52] Y.-F. Xiao, Z.-F. Han, Y. Yang, and G.-C. Guo, Phys. Lett. A **330**, 137 (2004).
[53] Y.-F. Xiao, X. M. Lin, J. Gao, Y. Yang, Z. F. Han, and G. C. Guo, Phys. Rev. A **70**, 042314 (2004).
[54] B. S. Ham, M. S. Shahriar, and P. R. Hemmer, Opt. Lett. **22**, 1138 (1997).
[55] B. S. Ham, P. R. Hemmer, and M. S. Shahriar, Opt. Commun. **144**, 227 (1997).
[56] K. Ichimura, K. Yamamoto, and N. Gemma, Phys. Rev. A **58**, 4116 (1998).
[57] A. V. Turukhin, V. S. Sudarshanam, M. S. Shahriar, J. A. Musser, B. S. Ham, and P. R. Hemmer, Phys. Rev. Lett. **88**, 023602 (2001).
[58] J. J. Longdell, E. Fraval, M. J. Sellars, and N. B. Manson, Phys. Rev. Lett. **95**, 063601 (2005).
[59] B. S. Ham and P. R. Hemmer, Phys. Rev. Lett. **84**, 4080 (2000).
[60] J. J. Longdell and M. J. Sellars, Phys. Rev. A **69**, 032307 (2004).
[61] J. J. Longdell, M. J. Sellars, and N. B. Manson, Phys. Rev. Lett. **93**, 130503 (2005).
[62] L. Rippe, M. Nilsson, S. Kröll, R. Klieber, and D. Suter, Phys. Rev. A **71**, 062328 (2005).
[63] C. C. Phillips, E. Paspalakis, G. B. Serapiglia, C. Sirtori, and K. L. Vodopyanov, Physica E (Amsterdam) **7**, 166 (2000).
[64] G. B. Serapiglia, E. Paspalakis, C. Sirtori, K. L. Vodopyanov,

and C. C. Phillips, Phys. Rev. Lett. **84**, 1019 (2000).
[65] M. C. Phillips *et al.*, Phys. Rev. Lett. **91**, 183602 (2003).
[66] K.-M. C. Fu, C. Santori, C. Stanley, M. C. Holland, and Y. Yamamoto, Phys. Rev. Lett. **95**, 187405 (2005).
[67] R. Kolesov, Phys. Rev. A **72**, 051801(R) (2005).
[68] R. Binder and M. Lindberg, Phys. Rev. Lett. **81**, 1477 (1998).
[69] U. Hohenester, F. Troiani, E. Molinari, G. Panzarini, and C. Mcchiavello, Appl. Phys. Lett. **77**, 1864 (2000).
[70] A. D. Greentree, J. H. Cole, A. R. Hamilton, and L. C. L. Hollenberg, Phys. Rev. B **70**, 235317 (2004).
[71] R. W. P. Drever *et al.*, Appl. Phys. B: Photophys. Laser Chem. **B31**, 97 (1983).
[72] M. Nilsson, L. Rippe, S. Kröll, R. Klieber, and D. Suter, Phys. Rev. B **70**, 214116 (2004).
[73] K. Holliday, M. Croci, E. Vauthey, and U. P. Wild, Phys. Rev. B **47**, 14741 (1993).
[74] R. W. Equall, R. L. Cone, and R. M. Macfarlane, Phys. Rev. B **52**, 3963 (1995).
[75] P. Meystre and M. Sargent III, *Elements of Quantum Optics* (Springer-Verlag, Berlin, 1999).
[76] F. R. Graf, A. Renn, G. Zumofen, and U. P. Wild, Phys. Rev. B **58**, 5462 (1998).
[77] It may be possible to fit the calculated result to the experimental result by choosing some parameters, such as γ_p, γ_p', and $W(\delta)$; but then, the values of the parameters are quite different from those reported before. Instead, we consider the effect of the neglect of the laser beam profile.